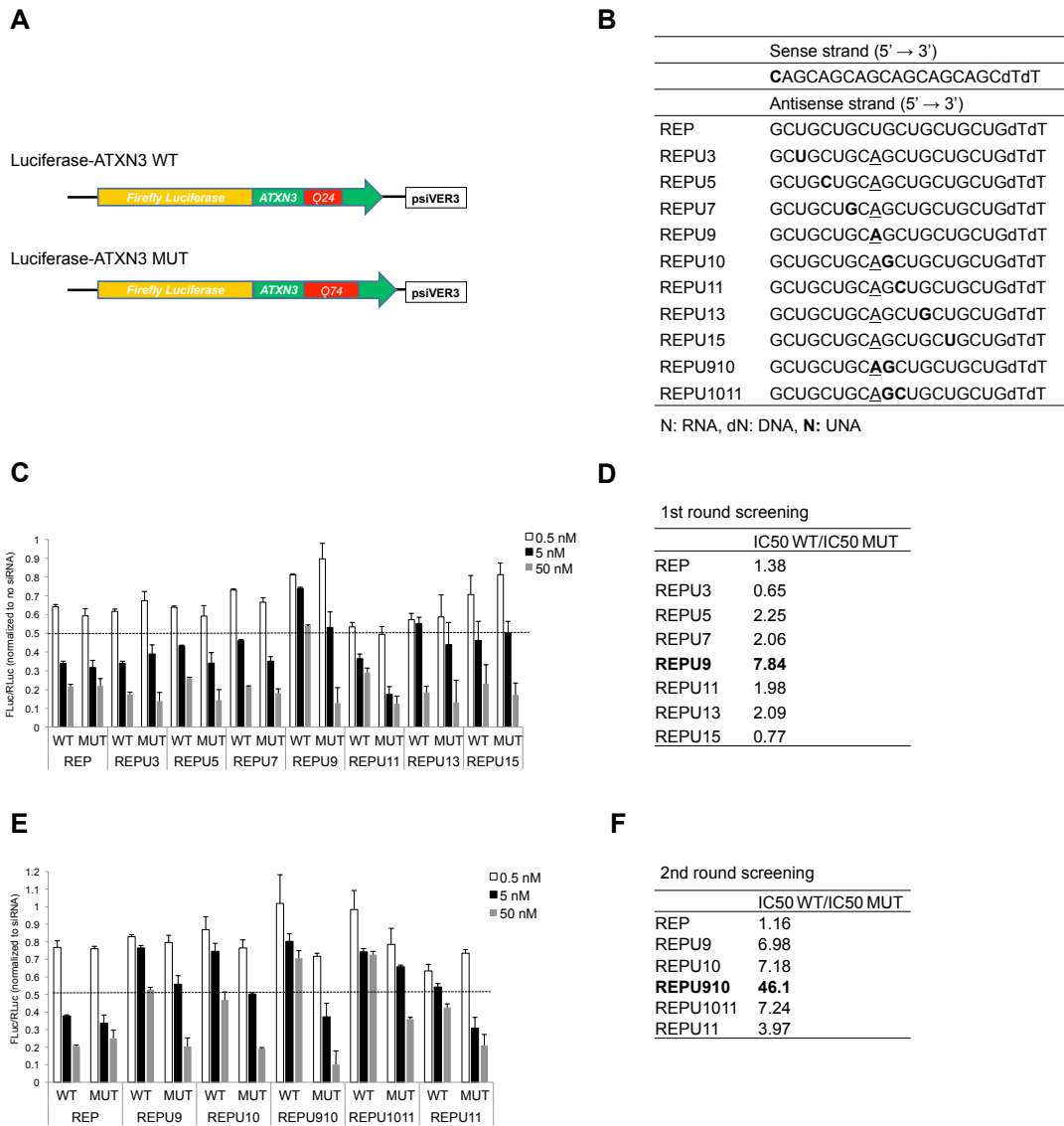


**Supplemental information**

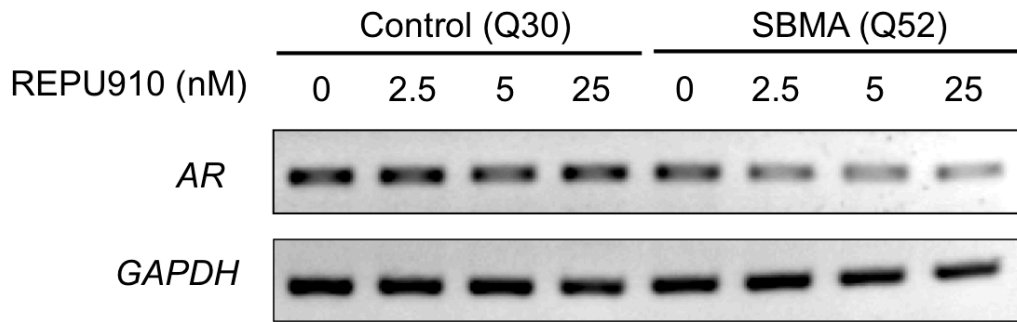
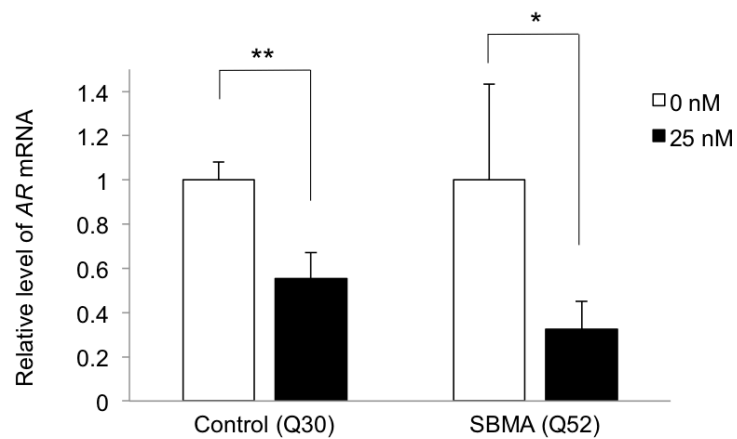
**Selective suppression of polyglutamine-expanded  
protein by lipid nanoparticle-delivered siRNA  
targeting CAG expansions in the mouse CNS**

**Tomoki Hironagi, Kentaro Sahashi, Kiyoshi Tachikawa, Angel I. Leu, Michelle Nguyen, Rajesh Mukthavaram, Priya P. Karmali, Padmanabh Chivukula, Genki Tohnai, Madoka Iida, Kazunari Onodera, Manabu Ohyama, Yohei Okada, Hideyuki Okano, and Masahisa Katsuno**



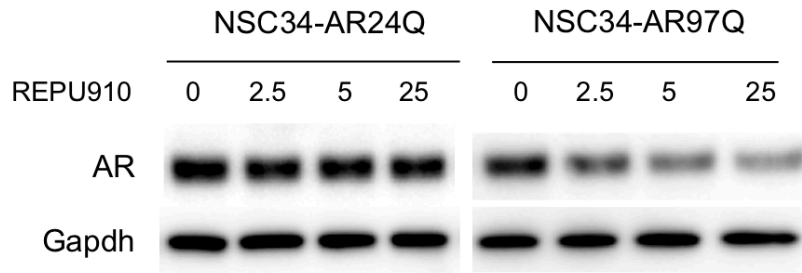
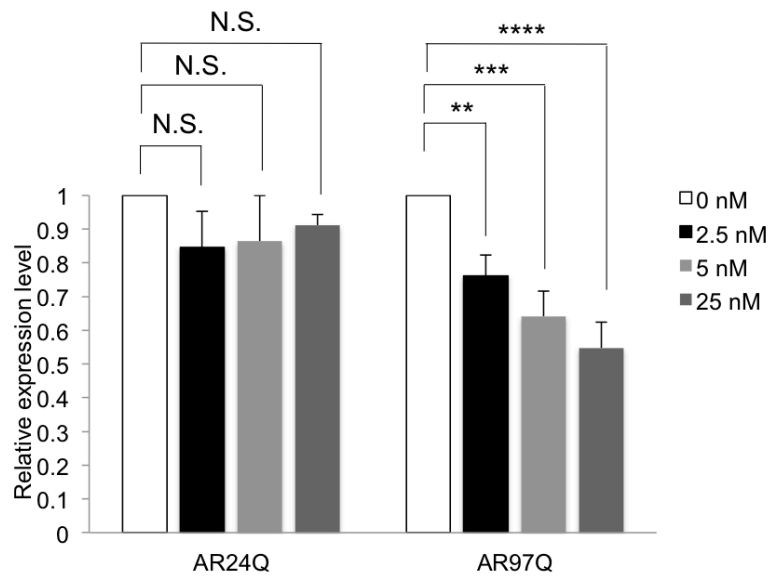
### Figure S1. Screening optimal UNA position in CAG-siRNA using luciferase-ataxin 3 reporter assay

(A) Scheme of luciferase-ataxin 3 (ATXN3) vectors. Wild-type (WT) and mutant (MUT) ATXN3 contain 24 and 74 CAG repeats, respectively. (B) The nucleotide sequences and chemical modifications of tested siRNAs. UNA substitutions are marked in bold. Underlining represents a central mismatch. (C) The normalized ratio of firefly to Renilla luciferase activity (FLuc/RLuc) in the first screening luciferase-ATXN3 reporter assay in HEK293 cells. (D) Selectivity (IC<sub>50</sub> WT/IC<sub>50</sub> MUT) of first round screening of siRNAs. (E) The normalized FLuc/RLuc in the second screening luciferase-ATXN3 reporter assay in HEK293 cells. (F) Selectivity (IC<sub>50</sub> WT/IC<sub>50</sub> MUT) of second round screening of siRNAs.

**A****B**

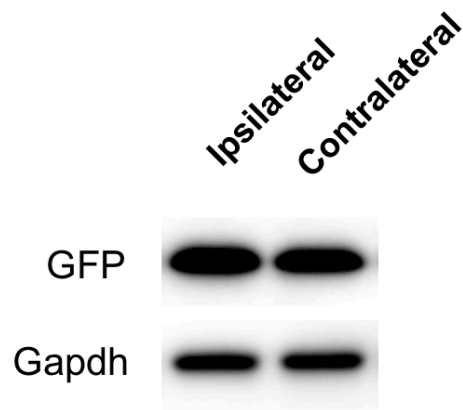
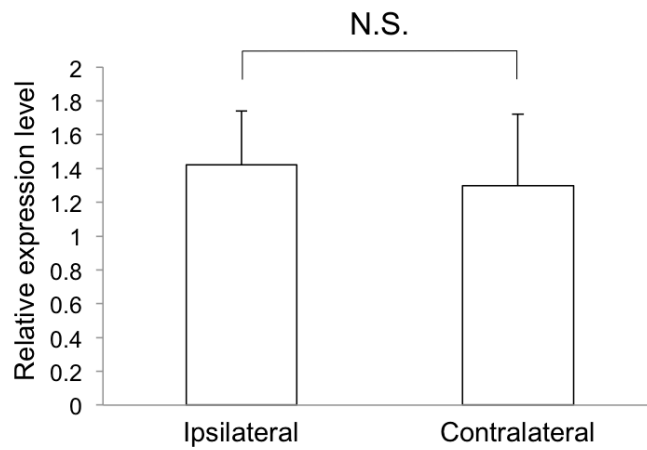
**Figure S2. Knockdown effect of REPU910 siRNA on AR mRNA levels in healthy control Q30 and SBMA Q52 fibroblasts**

(A) REPU910 siRNA suppresses AR mRNA levels and shows a similar tendency of its effect on protein levels (shown in Figure 1D). (B) Quantitative PCR analysis of AR mRNA levels after transfection with 0 or 25 nM REPU910 siRNA ( $n = 3$ , \*  $p < 0.05$ , \*\*  $p < 0.01$ ).

**A****B**

**Figure S3. Selective suppression of polyglutamine-expanded androgen receptor by REPU910 siRNA in NSC34 motor neuron-like cells**

(A) Knockdown effect of REPU910 siRNA (0, 2.5, 5, and 25 nM) on AR protein levels in NSC34 expressing wild-type (24Q) and mutant (97Q) AR. (B) Densitometric quantitation of AR band intensities shown in (A) ( $n = 3$  for each concentration, N.S.: not significant, \*\* $p < 0.01$ , \*\*\* $p < 0.001$ , \*\*\*\* $p < 0.0001$  One-way ANOVA with post-hoc Dunnett's test).

**A****B**

**Figure S4. Expression levels of eGFP in the ipsilateral and contralateral cerebral hemispheres of LUNAR-eGFP-injected mice**

(A) Western blot analysis of eGFP protein in the ipsilateral and contralateral cerebral hemispheres of LUNAR-eGFP (1800 ng)-injected mice. (B) Densitometric quantitation of eGFP band intensities shown in (A) (n = 4, N.S.: not significant, two-sided paired t test).

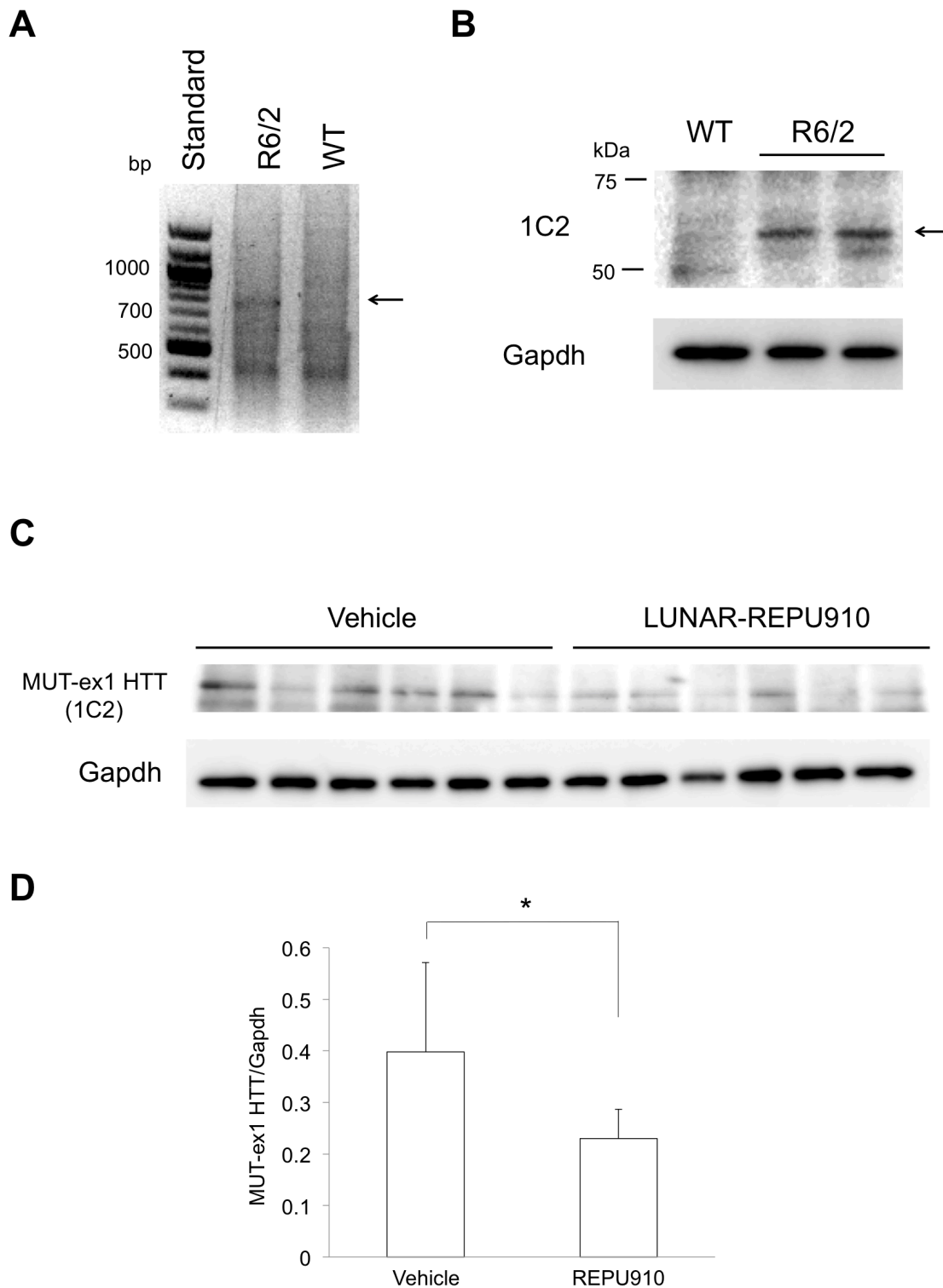


**Figure S5. LUNAR-REPU910 suppressed mutant exon 1 huntingtin in the CNS of R6/2 HD model mice**

(A) PCR analysis of tail genomic DNA for the determination of the CAG repeat lengths shows a band between 700 and 800 bp (arrow), indicating that R6/2 mice used in this study harbor mutant exon 1 huntingtin (MUT-ex1 *HTT*) with approximately 160–190 CAG repeats. (B) Detection of MUT-ex1 HTT protein by Western blot analysis using 1C2 antibody (arrow). (C) Western blot analysis of MUT-ex1 HTT protein in the temporal cortex of LUNAR-REPU910 (1800 ng)-injected R6/2 mice. (D) Densitometric quantitation of MUT-ex1 HTT band intensities shown in (C) ( $n = 6$ , \*  $p < 0.05$ ).